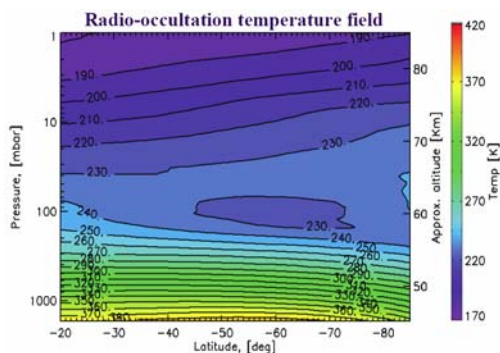


**Introduction:** Venus Express is the first European (ESA) mission to the planet Venus. It aims at the global and long-term remote survey of the atmosphere and the plasma environment and thermal mapping of the surface from orbit. The spacecraft, based on the Mars Express bus modified for the conditions at Venus, provides a versatile platform for nadir and limb observations as well as solar, stellar, and radio occultation. The payload consists of seven experiments and includes a powerful suite of imagers and spectrometers, instruments for in-situ analysis of the planetary plasma, and a radio science experiment [1, 2]. Since April 2006 Venus Express has been performing detailed observations of the Venus atmosphere providing new and deep insight in the physics of our mysterious sister-planet and significantly contributing to the field of comparative planetology. Here we present the highlights of the Venus Express atmospheric observations during 3 years of the nominal and extended missions recently published in the special issue of Journal Geophysical Research-Planets [3].

**Temperature structure:** Venus Express uses three remote sensing techniques for temperature sounding: thermal emission spectroscopy in 4.3  $\mu\text{m}$  CO<sub>2</sub> band, radio- and stellar occultation [4, 5]. They cover altitude range from 140 km to 40 km at all latitudes. From equator to pole the atmospheric temperature increases above 70 km and decreases below 60 km with “cold collar” in between characterized by deep temperature inversions at the cloud tops (fig. 1). The atmosphere was found to be convectively unstable within the main cloud deck (50-60 km) and stable above and below this region.



**Figure 1:** Temperature field from radio-occultation [4].

**Atmospheric composition:** Venus Express uses two novel techniques to study the atmospheric composition. SPICAV/SOIR acquires high-resolution ( $\lambda/\Delta\lambda \sim 20,000$ ) spectra of the Venus atmosphere in solar occultation geometry [6], providing vertical profiles of atmospheric trace gases in the meso-

sphere (70-110 km). VIRTIS exploits the potential of deep atmosphere sounding by mapping the dark side in spectral transparency “windows” at 0.9-5.0  $\mu\text{m}$  [7]. Figure 2 shows the summary of Venus Express composition investigations.

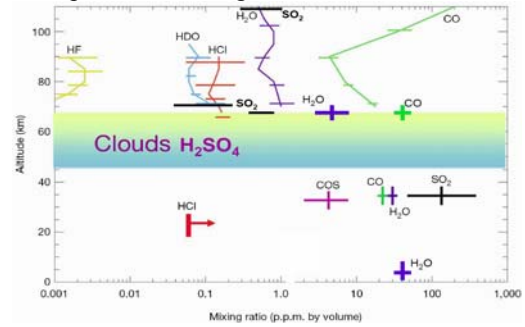


**Figure 2:** Summary of the Venus Express composition results[2].

**Cloud morphology and dynamics:** The imaging experiments VIRTIS and VMC monitor the cloud morphology in the broad spectral range from UV to thermal IR thus sounding different altitudes within the cloud deck (fig. 3) [8, 9]. The observations suggest that convective and eddy processes dominate in the tropics giving way to non-turbulent flow at high latitudes. Temperature and dynamic conditions at the cloud tops were found responsible for the observed global UV pattern [10]. Mapping the cloud top altitude discovered global depression in the polar region [11].

The general circulation has vortex organization with its “eye” at the pole (fig. 3) [12]. Wind velocities derived at 70-50 km from tracking cloud features are almost constant up to  $\sim 50\text{S}$  and quickly fade out to the pole [13, 14] in general agreement with the cyclostrophic balance in the middle latitudes [2].

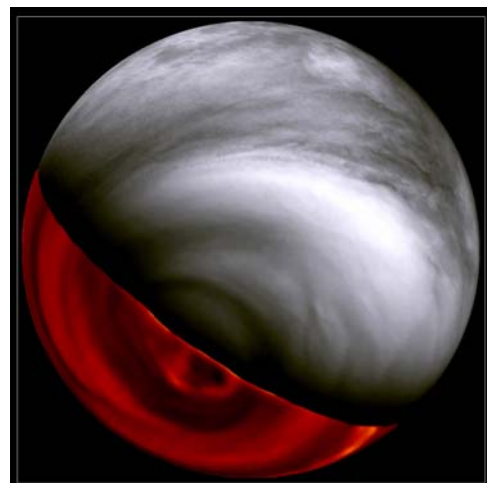


**Figure 3:** Composite of the VMC UV image of the day side (grey) and VIRTIS near-IR image of the night side (red).

**Atmospheric escape:** Plasma investigations by magnetometer and ASPERA experiments indicated that the ion escape occurs mainly through the plasma wake [15]. The main escaping ions are  $O^+$ ,  $H^+$ , and  $He^+$  with  $H^+/O^+ \sim 2$  – stoichiometric ratio of water. These observations have important implications for the evolution of the Venus atmosphere and the role of magnetic field.

**Surface investigations:** Venus Express studied the surface by two techniques. Bi-static radar sounding confirmed earlier detection of high dielectric material ( $4 < \epsilon < 25$ ) in the elevated regions of Maxwell Montes [16]. Unfortunately the failure of 13 cm radio channel in summer of 2007 precluded further radar investigations. VIRTIS and VMC performed systematic thermal mapping of the surface in the  $1 \mu m$  transparency window on the night side. VIRTIS acquires mosaics of the Southern hemisphere from apocentre and the ascending branch of the orbit. VMC takes close-up images of the equatorial region when the spacecraft is in eclipse. Figures 4 and 5 show examples of the VMC mosaics [17]. The brightness contrasts in the images are caused by variations in surface temperature due to topography and to a lesser extent by emissivity changes. Major relief features are clearly recognized in the figures, although spatial resolution is severely degraded to  $\sim 50$  km at best by scattering in the thick atmosphere.

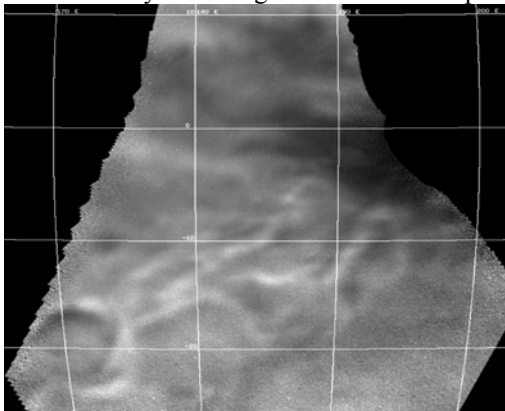


Figure 4: VMC mosaic of the rift zone south-west between Ozza Mons and Atahensik Corona.

Analysis of the VIRTIS data showed that surface emissivity variations reach about 10% (Fig. 6) [18, 19]. Tesserae were found to have lower emissivity, while some volcanic edifices and large lava flows in Lada Terra and Lavinia Planitia showed increased emissivity. This might indicate a more felsic surface composition of tesserae highlands and large scale extrusive volcanism of ultramafic composition. Visual inspection of the VMC images for potential volcanic activity so far has not revealed any sign of lava flows large and hot enough to be detected.

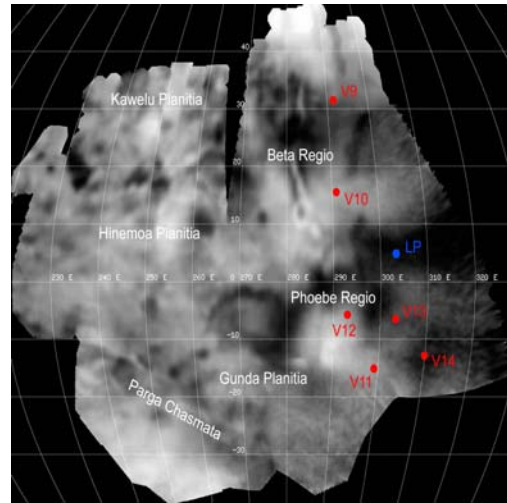


Figure 5: VMC mosaic of the Beta and Phoebe region and Hinemoa Planitia. Colour dots show landing sites of Venera and Pioneer Venus descent probes.

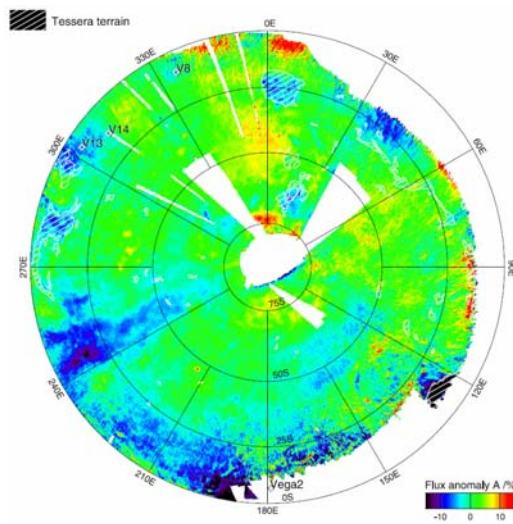


Figure 6: VIRTIS map of  $1 \mu m$  flux anomaly. Hatched areas indicate tessera terrains with negative flux anomaly (low emissivity).

**References:** [1] Svedhem, H. et al. (2009) *JGR*, 114, E00B33. [2] Titov, D. et al. (2009) *Solar Sys. Res.*, 43, 185-209. [3] Titov, D. et al. (2008) *JGR*, 113, E00B19. [4] Tellmann, S. et al. (2008) *JGR*, 114, E00B36. [5] Grassi, D. et al. (2008) *JGR*, 113, E00B09. [6] Vandaele, A.C. et al. (2008) *JGR*, 113, E00B23. [7] Marcq, E. et al. (2008) *JGR*, 113, E00B07. [8] Markiewicz, W.J. et al. (2007) *Nature*, 450, 633-636. [9] Piccioni, G. et al. (2007) *Nature*, 450, 637-640. [10] Titov, D. et al. (2008) *Nature*, 456, 620-623. [11] Ignatiev, N. et al. (2009) *JGR*, 114, E00B31. [12] Limaye, S. et al. (2009) *GRL*, 36, L04204. [13] Moissl, R. et al. (2009) *JGR*, 114, E00B31. [14] Sanchez-Lavega et al. (2008) *GRL*, 35, L13204. [15] Barabash, S. et al. (2007) *Nature*, 450, 650-653. [16] Simpson et al. (2009), *JGR* 114, E00B41. [17] Basilevsky et al. (2009), *JGR (submitted)*. [18] Mueller et al. (2008), *JGR* 113, E00B17. [19] Arnold et al. (2008), *JGR* 113, E00B10.